

DIFFERENTIAL SCALING OF CRATERING PHENOMENA: CONSEQUENCES FOR CRATER MORPHOLOGY; M.J. Cintala¹ and R.A.F. Grieve²; ¹Code SN21, NASA JSC, Houston, TX 77058; ²Geological Survey of Canada, Geophys. Div., Ottawa, Ontario K1A 0Y3.

The difficulties in reconciling calculations of impact-melt and crater volumes as calculated by various computational techniques and scaling laws have been discussed by a number of investigators.^{1,2,3} The principal variables controlling melt and vapor volumes are the target and impactor densities, impact velocity, and impactor radius; while crater dimensions also depend on these same factors, gravitational acceleration (g) exerts an important influence in governing the final cavity size.⁴ The impactor radius and g are very important in that, as larger projectiles or higher gravitational accelerations are considered, the melt and crater volumes will increase at different rates, with the result that the ratio of melt volume to crater volume generally will grow with the magnitude of the event.^{1,2,3} Some of the particulars of this relationship are addressed here, and some suggestions are offered regarding potential consequences for crater morphology and cratering mechanics.

The Impact Model: Thermodynamic calculations similar to those used earlier⁵ are employed here with some modifications. Phase changes are determined by calculating the increase in entropy at different points on the material's Hugoniot, using a modified Murnaghan equation of state. To approximate off-axis shock decay as observed in the more detailed finite-difference models,^{6,7,8} the shock stress varies as a function of $\cos^{2\beta}\theta$, where β is the ratio of target to projectile compression, and θ is the angle from the axis to the point of interest in the target (as measured from the center of the stress field). The energy contained in the shock is dependent only on its initial value at detachment and on losses to entropy in the target. Unlike that of Gault and Heitowitz,⁹ this model does not assume constant energy behind the shock front. As a result, the decay of shock stress with distance into the target is similar to those found in finite-difference calculations,⁶ as are the resulting melt and vapor volumes. Unless specified otherwise, the term "melt" will be used below to include all material with sufficient post-shock internal energy to begin fusing the target material.

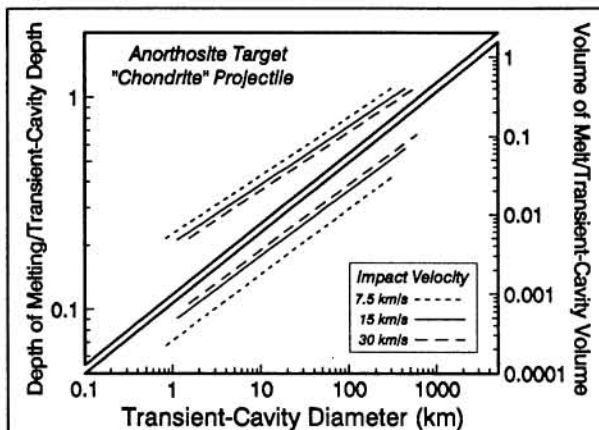


Figure 1. Depth of melting (left) and volume of melt (right) relative to the depth and volume of the transient cavity, respectively, as a function of the transient-cavity diameter. Each parameter is plotted for three different impact velocities.

Crater Dimensions: A modified version¹⁰ of the relationship for scaling craters in hard rock as given by Schmidt¹¹ is used here to estimate the volumes of transient cavities. As the cavity depths determined from a combination of this relationship and a similar one for crater diameter¹¹ are at variance with those observed in the field,¹² it was assumed that all transient cavities possess parabolic cross-sections with a fixed depth-diameter (d_{tc}/D_{tc}) ratio of 0.33. The diameter is then a derived quantity, found from simultaneous consideration of the cavity volume and the d_{tc}/D_{tc} ratio. Calculations were performed for vertical impacts of "chondrites" (simulated with a 3.58-g/cm³ "basalt") into anorthosite at lunar g (162 cm/s²). Although few planetary impacts occur normal to the target surface,¹³ oblique impact angles will change only the symmetry of the craters discussed below. Velocities ranged from 7.5 to 30 km/s and projectile diameters from 25 m to 50 km.

Discussion -- The Role of Melting: The effects of increasing event magnitude on the volume of melt and depth of melting relative to that of the transient cavity are illustrated in Fig. 1. The volumes of melt generated on the Moon relative to the associated cavity are smaller than in the terrestrial case by a factor of about 3, owing to the different values of g .¹⁴ Nevertheless, at impact velocities typical of the present-day Moon (~14 km/s),¹⁵ the depth of melting d_m would approach the depth of the transient cavity d_{tc} even for common crater sizes (100 - 200 km; Fig. 1). This effect would occur at correspondingly smaller diameters if shallower cavities were the case; values of $d_m/d_{tc} > 1$ will also occur with other crater-scaling relationships,^{4,12} although the critical diameters will be somewhat different. Thus, given the significant depths of melting in Fig. 1, fusion-induced modification of transient-cavity geometry appears to be unavoidable on the Moon, the Earth,¹⁴ and, by inference, the other terrestrial planets. Even if melting were not to extend to the base of the cavity, wholesale fusion of displaced (*i.e.*, not ejected) material would occur in relatively small events. **Morphological Implications:** Many important morphological elements occur in crater interiors, particularly on their floors. Perhaps the most diagnostic and stubbornly enigmatic class of such features

DIFFERENTIAL SCALING AND CRATER MORPHOLOGY: Cintala, M.J and Grieve, R.A.F.

are the central structures. Since impact melting and crater size scale differently, it is reasonable to consider their possible combined influence on the morphologies of central structures. The effects of this interaction at relatively small diameters should be minimal,¹⁶ but more drastic consequences would be experienced by increasingly larger craters (Fig.2). The depth of melting will equal and surpass the depth of excavation at crater sizes near the simple-complex transition on the Moon (~20 km). In larger events, the floor of the cavity itself will suffer intense melting, and portions of the rebounding, originally displaced material would become increasingly weaker due to the greater component of melted material. Single, large central peaks would very likely "fragment" into multiple massifs in larger events; extensive fusion of the central area would yield isolated peaks in a rough ring. A truly large impact would induce wholesale melting of large volumes at and well below the base of the cavity, resulting in a well-defined peak ring upon cavity readjustment and, hence, a peak-ring basin. It is relevant to note here that no large peak-ring basin has been observed without extensive interior deposits of impact melt, unless they are buried by subsequent volcanic deposits. Such large-scale melting at depth would have profound consequences in many areas, including cavity modification and subsequent evolution, petrology, and geophysics. The documented evolution of the morphology of central structures as a function of final crater diameter would thus be a straightforward consequence of differences in the scaling of impact-melt and cavity volumes.

References: 1 Croft, S.K. (1983) *PLPSC 14*, JGR 88, B71. 2 Cintala, M.J. and Grieve, R.A.F. (1984) *LPS 15*, 156. 3 Melosh, H.J. (1989) *Impact Cratering: A Geologic Process*, Oxford, 245pp. 4 Schmidt, R.M. and Housen, K.R. (1987) *Int. J. Impact Eng.* 5, 543. 5 Cintala, M.J. (1984) *LPS 15*, 154. 6 O'Keefe, J.D. and Ahrens, T.J. (1977) *PLPSC 8*, 3357. 7 Austin, M.G. et al. (1979) *PLPSC 11*, 2325. 8 Orphal, D.L. et al. (1980) *PLPSC 11*, 2309. 9 Gault, D.E. and E.D. Heitowit, *Proc. 6th Hypervel. Impact Symp.*, 419. 10 M.J. Cintala and R.A.F. Grieve, this volume. 11 Schmidt, R.M. (1980) *PLPSC 11*, 2099. 12 Dence, M.R. et al. (1977) *Impact and Explosion Cratering* (D.J. Roddy, R.O. Pepin, and R.B. Merrill, eds.), Pergamon, 247. 13 Gault, D.E. and Wedekind, J.A. (1978) *PLPSC 9*, 3843. 14 Grieve, R.A.F. and Cintala, M.J., this volume. 15 Hartmann, W.K. (1977) *Icarus 31*, 260. 16 Hawke, B.R. and Head, J.W. (1977) *LS VIII*, 415. 17 D.E. Maxwell (1977) *Impact and Explosion Cratering* (D.J. Roddy, R.O. Pepin, and R.B. Merrill, eds.), Pergamon, 1003. 18 R.A.F. Grieve (1988) *Meteoritics 23*, 249. 19 Hale, W.S. and Grieve, R.A.F. (1982) *PLPSC 13*, JGR 87, A65.

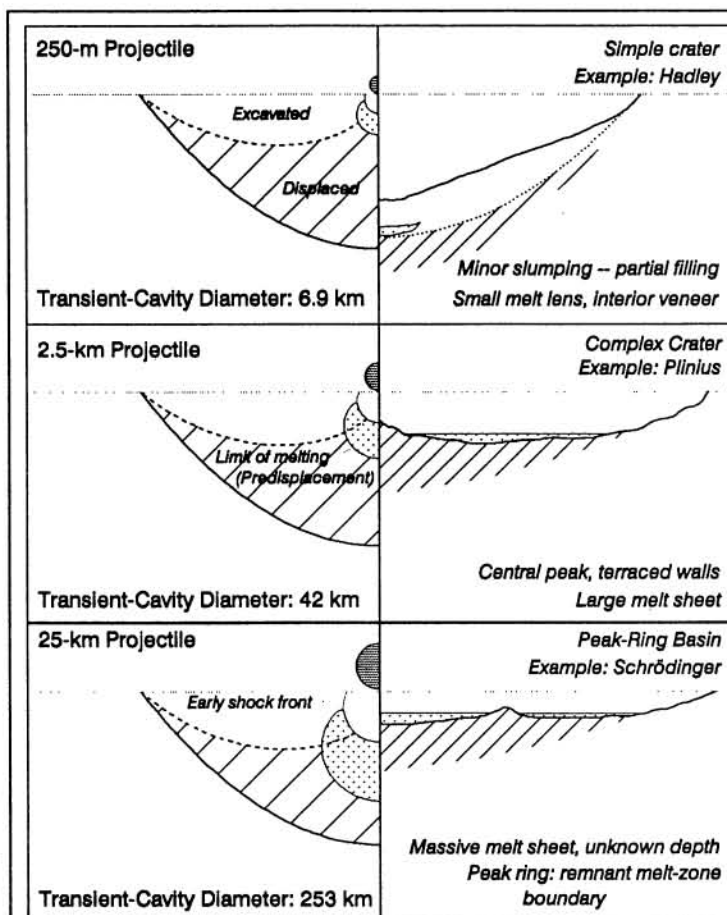


Figure 2. Schematic representation of the possible effects of impact melting on crater morphology; the impact velocity was held constant at 15 km/s for each panel in this figure. This idealized illustration is constructed such that the transient cavities are drawn with a fixed size in the left-hand panels, thus permitting a visual assessment of the increase in relative melt volume as the size of the event increases. The curve separating the ejected and displaced volumes is a streamline ($Z=2.7$) from Maxwell's Z-model.¹⁷ Although there is some evidence against the applicability of a simple Z-model to large craters,¹⁸ it is included here to delineate the difference between the ejected and displaced volumes. Profiles of the resulting craters after modification are shown on the right; rim structure above the original target surface is not depicted. The configuration below the center of the peak-ring basin is open to debate; an important feature of this model, however, is the formation of the peak-ring itself as the "cusp" formed by the melt boundary and unmelted, displaced mass. Due to strongly divergent flow during excavation, it is likely that the cusp will be more poorly defined than it is in this idealized illustration; see, for example, the peak ring of Schrödinger basin.